Kinetics and Catalysis, Vol. 44, No. 6, 2003, pp. 778–787. Translated from Kinetika i Kataliz, Vol. 44, No. 6, 2003, pp. 849–859.

Esterification of *n*-Butanol with Acetic Acid in the Presence of $H_3PW_{12}O_{40}$ Supported on Mesoporous Carbon Materials

M. N. Timofeeva, M. M. Matrosova, G. N. Il'inich, T. V. Reshetenko, L. B. Avdeeva, R. I. Kvon, A. L. Chuvilin, A. A. Budneva, E. A. Paukshtis, and V. A. Likholobov

Boreskov Institute of Catalysis, Siberian Division, Russian Academy of Sciences, Novosibirsk, 630090 Russia

Received October 22, 2002

Abstract—The adsorption of $H_3PW_{12}O_{40}$ (HPA) from methanol solutions on mesoporous carbon supports (multiwall carbon nanotubes (CFC-3) and CFC modified with nitrogen atoms (N-CFC)) was studied. It was found that up to 10 wt % HPA was irreversibly adsorbed on the surface of CFC. This character of adsorption is indicative of the strong interaction of the adsorbate (HPA molecules) with coal surface groups (carboxylic, lactone, etc.) to form intermolecular hydrogen bonds with π-electron interactions. It was found that N-containing surface centers affected the adsorption of HPA on N-CFC. The acid and catalytic properties of HPA/CFC systems in the esterification reaction of *n*-butanol with acetic acid were studied ([BuOH]/[HOAc] = 1 : 15 mol/mol; 80°C). It was found that the strength of proton centers, which was determined as proton affinity, decreased upon supporting HPA. The HPA/CFC-3 systems most actively catalyzed the reaction. The catalytic activity of HPA/N-CFC depended on the nature of N-containing groups at the support surface, and it decreased with concentration of pyridine-like structures.

INTRODUCTION

Heteropoly acids (HPAs), which are strong Brønsted acids, are widely used as homogeneous and heterogeneous acid catalysts [1, 2]. Interest in supported HPAs has increased in the past few years because their activity is often higher than the activity of bulk HPAs [2–5].

Many porous materials are widely used as supports for HPAs. The adsorption of HPAs with the Keggin structure (primarily, $H_3PW_{12}O_{40}$ and $H_4SiW_{12}O_{40}$) on various supports has been studied systematically. It was found that, on the surfaces of many supports, HPAs underwent partial or complete degradation (SiO_2, activated carbons, MgF_2, and Al_2O_3) or entered into various chemical reactions with the supports to form HPA salts [5–7]. Moreover, the acid sites of adsorbed HPAs weakened in the following order of supports: SiO_2 > Al_2O_3 > activated carbon [5–7]. In the case of HPA/activated carbon, the weakening of acid sites on the carbon surface is most likely due to the strong interaction of HPA molecules with the surface groups of carbon. This is evidenced by the irreversible adsorption of HPAs in an amount of ~5–10% (on a support basis) on carbons [5–7]. Although the acidity of proton centers is reduced, HPA/activated carbon systems are sufficiently active catalysts for a number of reactions (the esterification of ethanol with acetic acid [5] and the dehydration of methanol [8, 9]).

Presently, a vast number of structurally different carbon materials are known. Catalytic fibrous carbon (CFC), which is prepared by the decomposition of hydrocarbons in the presence of catalysts based on iron subgroup transition metals, occupies a prominent place among these materials. The structural and textural characteristics of CFC can be purposefully changed by varying the conditions of the synthesis, the nature of the metal, the dispersity of metal particles at which nanofibers are grown, the composition of hydrocarbon raw materials, and the conditions of hydrocarbon decomposition [10]. Because of its mesoporous structure, CFC is considered a promising material for use in the adsorption–catalytic conversion of bulky substrates. Previously [11], the adsorption of $H_3PW_{12}O_{40}$ on the surface of CFC, which was prepared by methane decomposition on a nickel–copper catalyst, was studied; the character of adsorption was found to be analogous to HPA adsorption on SiO_2.

The fixation of nitrogen heteroatoms on the surface of porous carbon materials, which results in the formation of C–N bonds in pyridine- and pyrrole-like structures, aromatic amines, and other N-containing groups, seems promising for the development of new functionally active sorbents and supports and a new class of catalysts. The simplest procedure for the modification of carbon materials consists in the treatment of their surface with NH_3 or HCN at temperatures up to 900°C [12–16]. However, spatially modified carbon materials [17–22], in which heteroatoms are the constituents of structure-forming associates of carbon atoms (because of which the physicochemical properties of the entire carbon skeleton can be changed), have attracted particular attention. These carbon materials can be prepared by the decomposition of N-containing hydrocarbon raw materials (heterocyclic compounds, such as pyridine (C_5H_5N) [20–22] and melamine ($C_3N_3(NH_2)_3$) [18, 19],

0023-1584/03/4406-0778$25.00

or acetonitrile (CH_3CN) [20, 21]) in vapor–gas mixtures with an inert gas, H_2, and/or hydrocarbons on metal catalysts (Ni, Co, and Fe).

Many publications were devoted to the XPS studies of the chemical states of nitrogen atoms in carbon matrices and on the surfaces of carbon materials [12–14, 22–25]. Based on semiempirical quantum-chemical calculations of a carbon cluster, Strelko *et al.* [26] predicted the effects of various N-containing groups (pyridine and pyrrole), as well as nitrogen atoms that replace carbon atoms in a hexagonal planar structure, on an increase in both the donor–acceptor properties of the surface and the catalytic activity of the modified carbon materials in electron-transfer reactions. These data are consistent with the experimental results obtained by Boehm and coauthors [12, 27], Jansen and van Bekkum [13], Li *et al.* [16], and Pels *et al.* [23]. The effect of nitrogen on the formation of basic coals with relatively high ion-exchange capacities was noted [15, 28].

The aim of this work was to study the synthesis of supported HPA/carbon (HPA/C) catalysts and to test their catalytic activity in the esterification reaction of *n*-butanol with acetic acid

$$BuOH + HOAc \rightleftharpoons BuOAc + H_2O. \quad (I)$$

The following new mesoporous fibrous carbon materials were used as supports for the catalysts: multiwall carbon nanotubes (CFC-3) and nitrogen-containing CFC (N-CFC).

Reaction (I) is of practical importance for the production of butyl acetate, which is widely used in organic synthesis [29].

EXPERIMENTAL

Reagents

Chemically pure $H_3PW_{12}O_{40} \cdot 15.41H_2O$ was recrystallized from water. HOAc of analytical grade; chemically pure *n*-butanol; and reagent-grade MeOH, *ortho*-xylene, decane, and hexane were used in this study without additional purification.

Preparation of Supports

Mesoporous CFC with a nanotubular structure (CFC-3) and N-CFC with different nitrogen contents were used as supports. CFC-3 was prepared by methane decomposition at 625°C with the use of an iron-containing catalyst. The samples of N-CFC were synthesized by the decomposition of an H_2–CH_4–N-containing additive (C_5H_5N or CH_3CN) vapor–gas mixtures on Ni–Cu metal catalysts at 550, 650, and 750°C. The catalysts were reduced *in situ* in a flow of H_2 immediately before the onset of decomposition of the reaction mixture. In the synthesis of N-CFC from H_2–C_5H_5N mixtures (molar ratio of 9 : 1) at 650°C (Table 1, sample nos. 2, 4, 5), the conditions of catalyst reduction were varied (temperature over the range 550–750°C and time from 1 to 2 h). As can be seen in Table 1, the conditions of catalyst reduction had almost no effect on the pore-structure parameters of N-CFC and on the nitrogen content of the samples. According to electron-microscopic data, the morphology of fibers also remained unchanged. At 750°C, H_2–C_5H_5N vapor–gas mixtures were decomposed by varying pyridine concentration in the initial reaction mixture (H_2/C_5H_5N molar ratios of 9 : 1 and 6 : 1; sample nos. 6 and 7,

Table 1. Characteristics of the carbon supports

No.	Carbon support	Conditions of preparation		Texture parameters			Nitrogen content, wt %	Adsorption of $H_3PW_{12}O_{40}$ from CH_3OH	
		composition of the starting material, mol %	T, °C	D_a, Å	S_{sp}, m^2/g	ΣV_{pore}, cm^3/g		a_{max}, mmol/g	a_{ib}, mmol/g
1	N-CFC(301)	C_5H_5N/H_2 (10 : 90)	550	53	282	0.4	1.0	0.086	0.038
2	N-CFC(259)		650	61	283	0.4	1.4	0.103	0.038
3	N-CFC(259)*		650	61	283	0.4	1.4	0.069	0.030
4	N-CFC(293)		650	50	309	0.4	1.4	–	–
5	N-CFC(295)		650	48	324	0.4	1.5	–	–
6	N-CFC(258)		750	79	290	0.6	2.7	0.103	0.038
7	N-CFC(286)	C_5H_5N/H_2 (15 : 85)	750	85	201	0.4	3.4	0.030	0.009
8	N-CFC(122)	CH_3CN/H_2 (15 : 85)	550	51	239	0.3	2.4	0.076	–
9	N-CFC(141)	$C_5H_5N/H_2/CH_4$ (10 : 20 : 70)	750	150	110	0.4	4.8	0.024	0.007
10	CFC-3	CH_4	625	129	125	0.4	0	0.054	0.028
11	CFC-3*		625	129	125	0.4	0	0.038	0.019

* Adsorption of $Na_3PW_{12}O_{40}$.

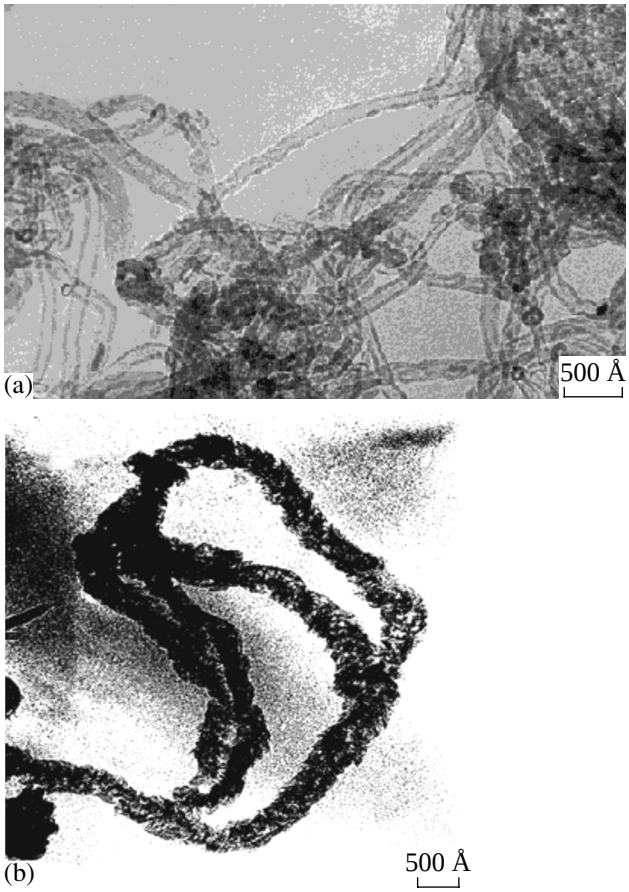

Fig. 1. Electron micrographs of (a) CFC-3 and (b) NCFC(141).

respectively). At a constant composition of the reaction mixture, an increase in the reaction temperature was accompanied by an increase in the nitrogen content of the carbon deposit. The procedures for the synthesis of CFC were described elsewhere [21, 22, 30]. Table 1 summarizes the main characteristics of the supports. All the supports were washed with methanol and dried in air. Pellets with a size of 0.5 mm were used.

HPA Adsorption on CFC

The adsorption of HPAs on CFC was studied in a thermostatted shaken reactor. The adsorbent (1 g) was loaded in the reactor and heated in a vacuum (10 Pa) at 120°C for 0.5 h. The reactor was cooled and 10 ml of an HPA solution in methanol ([HPA] = 10–150 g/l) was poured into it; the contents were allowed to stand until the establishment of equilibrium at atmospheric pressure and 25°C (the time of equilibration was < 2 h). The samples of the solution (0.1 ml) were taken at regular intervals, and the HPA concentration in the solution was measured, after dilution, with the use of a Specord UV-VIS M-40 spectrophotometer (ν = 32000–42000 cm^{-1}; determination error of ±10%). In the study of HPA desorption from the support, 10 ml of the pure solvent or an HPA solution with a concentration lower than equilibrium was added to 1 g of HPA/CFC. The equilibration time was < 2 h. The limiting values of HPA adsorption (a_{max}) were determined from adsorption isotherms at a region where the adsorption curve flattened out. The irreversible adsorption value (a_{ib}) was determined by boiling 1 g of the HPA/C sample in 20 ml of the pure solvent followed by separation from the solvent using vacuum filtration and ignition at 800°C in a muffle furnace. The value of a_{ib} was determined from the amount of the solid residue.

Preparation of HPA/CFC Catalysts

The supported HPA/CFC catalysts were prepared by $H_3PW_{12}O_{40}$ adsorption from a methanol solution. The support was kept in the HPA solution in methanol for 2 h; thereafter, it was filtered off, washed with methanol, and dried in air. Before use, the catalysts were calcined in air at 100°C for 2 h.

Kinetic Measurements

Esterification reaction (I) was performed in an aqueous acetic acid solution in a thermostatted glass reactor equipped with a magnetic stirrer and a reflux condenser. The reactor was loaded with HOAc, BuOH, and H_2O (molar ratio [BuOH]/[HOAc]/[H_2O] = 1 : 15 : 0.05), and the mixture was heated to 80°C. Next, the HPA/CFC catalyst was added in an amount of 3 wt % on a basis of the entire reaction mass. Samples were taken at regular intervals; the catalyst was removed by shaking with an *ortho*-xylene–water mixture (1 : 5, by volume), and the organic layer was analyzed by GLC. A Tsvet-500 chromatograph with a metal column (2 m × 3 mm) packed with 5% SE-30 on Chromaton AW-DMCS (0.16–0.25 mm) was used; nitrogen was the carrier gas (30 ml/min). The column temperature was 50°C; hexane was an internal standard, and a flame-ionization detector was used. Under conditions of a considerable excess of HOAc, the buildup of the reaction product, butyl acetate, obeyed the rate equation for a reversible first-order reaction. On this basis, the rate constants of the reaction were calculated from the ln[BuOAc] – τ linear anamorphosis, where τ is the reaction time.

Physicochemical Characterization of Supports and Catalysts

The pore structure of the supports was determined from the adsorption isotherm of nitrogen (77 K); the specific surface area (S_{sp}) of the samples was determined by the BET method. The average pore size was calculated from the equation $D_a = 4V_{pore}/S_{sp}$.

The samples of powdered $H_3PW_{12}O_{40}$/CFC for IR-spectroscopic studies were sprayed onto a NaCl plate. The IR spectra were measured on a Shimadzu FTIR

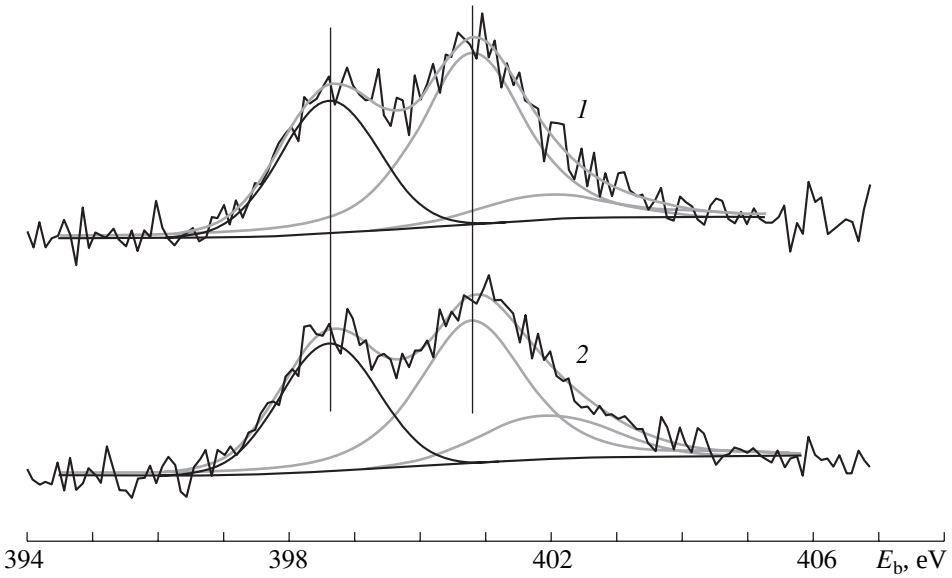

Fig. 2. XPS N 1*s* spectra of (*1*) N-CFC(293) and (*2*) N-CFC(295) samples.

8300 spectrometer in the frequency region 700–1800 cm^{-1} with a resolution of 4 cm^{-1}.

Samples for transmission electron microscopy (TEM) were prepared by the ultrasonic dispergation of $H_3PW_{12}O_{40}$/CFC in hexane followed by applying the suspension to a standard electron-microscopic grid coated with a carbon film. The samples were examined on a JEM-2010 instrument.

The XPS study of N-CFC was performed on a VG ESCALAB HP photoelectron spectrometer with the use of MgK_α and AlK_α primary radiation at a background gas pressure of 2×10^{-8} mbar. The spectrometer was calibrated against the positions of Au4$f_{7/2}$ (84.0 eV) and Cu2$p_{3/2}$ (932.7 eV) lines, and the internal standard method was used to take charging into account (carbon peak with a binding energy of 284.4 eV). Sample pellets were pressed in a double-sided adhesive tape, which was fixed in a standard sample holder.

RESULTS AND DISCUSSION

Characterization of Supports

It is well known that the carbon fibers of CFC grow at the active centers of a catalyst; in the course of this growth, they randomly interlace to form a carbon material granule as a three-dimensional matrix. In this case, the mesoporous volume of CFC is formed by hollows between individual nanofibers. According to electron-microscopic data, CFC-3 consists of multiwall carbon nanotubes, which include 7–15 graphite-like layers arranged in parallel with the fiber axis as cylinders with increasing diameters, which are embedded in one another (Fig. 1a). The diameter of nanotubes is 25–30 nm, whereas the size of the inner hollow channel is 10 nm. Partition walls were formed within carbon nanotubes because of closing graphite layers. The partition walls are oriented perpendicular to the fiber axis. According to electron-microscopic data, fibers as porous filaments (up to 90 wt %) are predominant in the structure of N-CFC (Fig. 1b); these fibers are formed of graphite-like carbon layers with a turbostratic structure.

Table 2. Surface characteristics of N-CFC according to XPS data

Sample	Binding energy of N 1*s*, eV		Surface composition, wt %			C_xNO_y	N_{Py}/N_S, %	$[N_{Py}]$, wt %
			Ni*	O	N*			
N-CFC(301)	398.4	400.7	1.06 (1.80)	3.2	1.0 (1.0)	$C_{68}NO_4$	53	0.53
N-CFC(293)	398.6	400.9	–	~1	1.0 (1.4)	$C_{103}NO_{0.9}$	37	0.37
N-CFC(295)	398.5	401.0	–	~1	1.0 (1.4)	$C_{118}NO_{0.8}$	40	0.40
N-CFC(286)	398.5	401.1	0.41	3.1	3.1 (3.4)	$C_{22}NO_{1.2}$	49	1.52
N-CFC(141)	398.8	401.0	0.43 (2.17)	4.0	4.3 (4.8)	$C_{26}NO_{1.2}$	45	1.94

* The elemental analyses of the samples are given in parentheses.

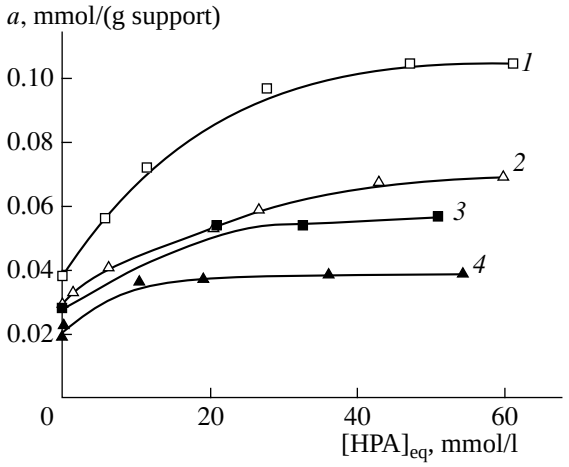

Fig. 3. Isotherms of adsorption from methanol solutions: (*1*) $H_3PW_{12}O_{40}$ on N-CFC(259), (*2*) $Na_3PW_{12}O_{40}$ on N-CFC(259), (*3*) $H_3PW_{12}O_{40}$ on CFC-3, and (*4*) $Na_3PW_{12}O_{40}$ on CFC-3.

The layers are perpendicular to the fiber axis at its central part. The ends of the basal planes of carbon outcropped at the surface of carbon fibers at an angle or almost parallel to the axis. The fibers are 15–150 nm in thickness. A special feature of the structure consists in its significant loosening: individual packs can be separated by gaps up to 1 or 2 nm. This is consistent with data on the low-temperature adsorption of nitrogen; according to these data, N-CFC samples can contain considerable amounts of micropores ($V_{micro} \le 7\%$ of the total pore volume). In this case, a change in the parameters of N-CFC synthesis, for example, an increase in the pyridine content of the initial reaction mixture (Table 1, sample nos. 6 and 7) or a decrease in the partial pressure of hydrogen with a CH_4–H_2 mixture in place of H_2 (Table 1, sample no. 9), was accompanied by a decrease in the specific surface area of N-CFC and by a reduction in the micropore volume up to the complete disappearance of micropores. One of the most important reasons for the above phenomenon is the occurrence of side reactions in the reaction system at temperatures higher than 600°C. These side reactions include the thermocatalytic conversion of pyridine, in particular, the dehydro-oligomerization of pyridine [22] followed by the slow pyrolysis of oligomers on the surface of carbon fibers. Even in the early 1990s, Downs and Baker [31] proposed the optimization of CFC synthesis conditions (temperature and hydrocarbon of choice) to eliminate undesirable side processes of uncatalyzed hydrocarbon polymerization to form disordered carbon, which can be accumulated in the structure of CFC.

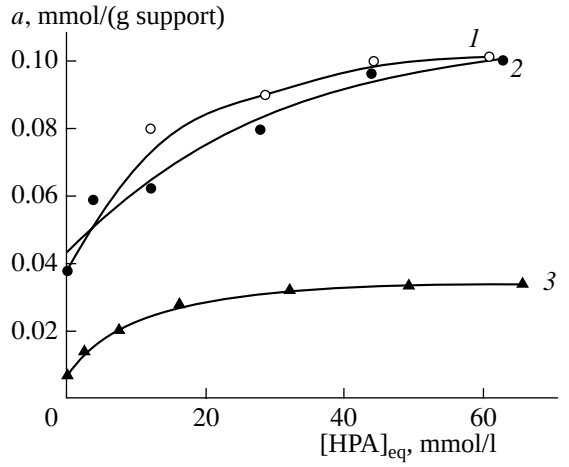

Fig. 4. Isotherms of $H_3PW_{12}O_{40}$ adsorption on N-CFC from methanol solutions: (*1*) N-CFC(259), (*2*) N-CFC(258), and (*3*) N-CFC(141).

The chemical composition of the surface of N-CFC was studied by XPS (Table 2). It was found that surface nitrogen can occur in at least two chemical states (Fig. 2). The N 1*s* peak with a binding energy (E_b) of 398.6 ± 0.2 eV belongs to the nitrogen atom N_{Py} in pyridine-like structures [12–25], which are localized at the lateral faces and defects of carbon layers, that is, primarily at the outer surface of nanofibers. The N 1*s* peak with E_b = 401 eV is a superposition of peaks with close binding energies (Fig. 2): it is most likely that a peak with E_b = 400.8 eV can be ascribed to the nitrogen atom of amine or aniline groups (C–NH_2, N_{Am}) [22] and/or protonated pyridine [26, 32], whereas a peak with E_b = 401.9 eV can be attributed to nitrogen that replaces a carbon atom in a

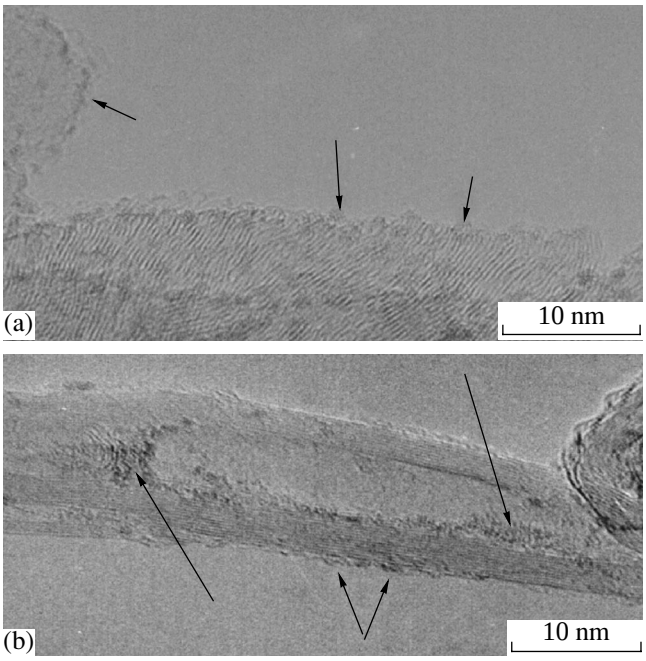

Fig. 5. Electron micrographs of $H_3PW_{12}O_{40}$ supported on mesoporous carriers: (a) 5.3% $H_3PW_{12}O_{40}$/CFC-3 and (b) 10% $H_3PW_{12}O_{40}$/N-CFC(259).

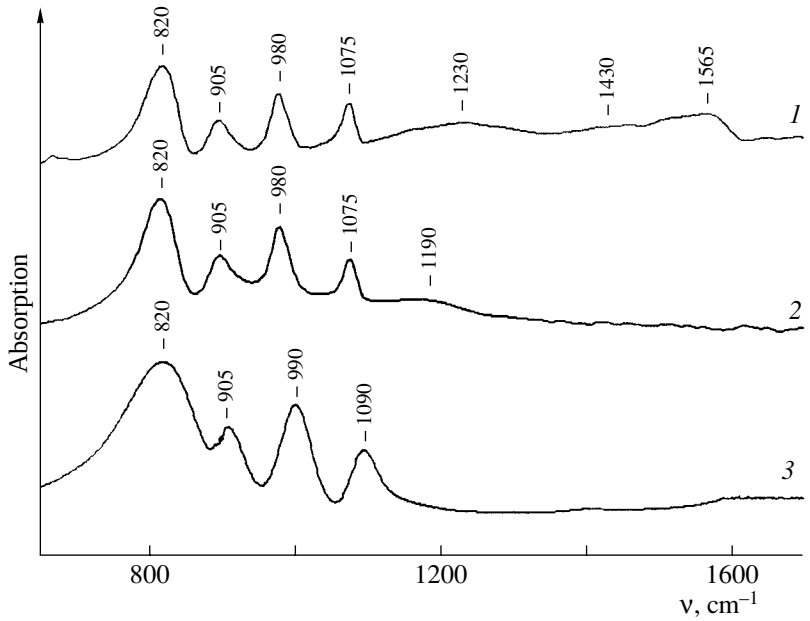

Fig. 6. IR spectra of bulk $H_3PW_{12}O_{40}$ and $H_3PW_{12}O_{40}$ supported on CFC of different origins: (*1*) 8% $H_3PW_{12}O_{40}$/CFC-3, (*2*) 10% $H_3PW_{12}O_{40}$/N-CFC(258), and (*3*) $H_3PW_{12}O_{40}$.

hexagonal planar structure (nitrogen inserted into graphene layers) [16, 25].

In addition to N-containing groups, a significant amount of adsorbed oxygen occurred on the surface of N-CFC (Table 2). Because the conditions of the synthesis of N-CFC completely excluded the contact of reactants and the resulting carbon deposit with oxygen, it is evident that the presence of O-containing groups can be explained by the adsorption of oxygen, water vapor, etc., on the surface of the supports in storage of the samples in air. The presence of great amounts of oxygen adsorbed on the surface of porous carbon materials is a well-known fact.

Adsorption of $H_3PW_{12}O_{40}$ on CFC

One of the most important requirements imposed on catalysts for liquid-phase reactions consists in the ease of catalyst separation from the reaction mass. In this context, an important stage of this work was the preparation of heterogeneous catalysts for reaction (I) based on $H_3PW_{12}O_{40}$ immobilized on the surface of mesoporous carbon materials with the use of an adsorption method.

Because the type of the support, the concentration of an initial HPA solution, and the nature of the solvent have a pronounced effect on the character of adsorption and the surface state of HPAs, we studied the adsorption of $H_3PW_{12}O_{40}$ by catalytic fibrous carbons of different chemical origins [2, 6, 11]. Methanol was chosen as a solvent to prevent HPA hydrolysis by the strongly basic N-containing surface groups of N-CFC.

Figures 3 and 4 demonstrate the shapes of HPA adsorption isotherms depending on the type of CFC. In all cases, the adsorption was partially irreversible: ~20–110 mg (0.007–0.038 mmol) of $H_3PW_{12}O_{40}$ per gram of support. The further adsorption was reversible, and the desorption curve coincided with the adsorption one. Table 1 summarizes the limiting values of HPA adsorption (a_{max}) and the irreversibly bound HPA (a_{ib}). It was noted [6, 11] that the complete desorption of HPA from the surfaces of CFC and activated carbon was impossible even upon boiling in water or methanol. This character of adsorption is usually indicative of the strong interaction of adsorbed molecules (HPA molecules) with the surface of the support [33–37]. Note that irreversible adsorption can also be due to the possibility of the encapsulation of bulky HPA molecules ("landing" surface area of 100 Å^2) [1] in the narrowest pores of the adsorbent because of the adsorption deformation of carbon. The adsorption deformation was easily observable in microporous carbon materials [38]; however, in the case of CFC, the issue of grain extension still remains open.

The concentrations of acidic (carboxylic, lactone, etc.) and basic groups that occurred on the surfaces of CFC-3 and N-CFC(259) were determined by back titration as described in [39]. The amounts of acidic groups were equal to 88 and 90 μmol/g for CFC-3 and N-CFC(259), respectively. The amount of basic groups in N-CFC(259) was equal to 120 μmol/g, whereas these groups were not detected in CFC-3. These data indicate that the interactions of HPA with the surface groups of the CFC-3 and N-CFC(259) supports exhibited some differences. In CFC-3, a weak intermolecular hydrogen

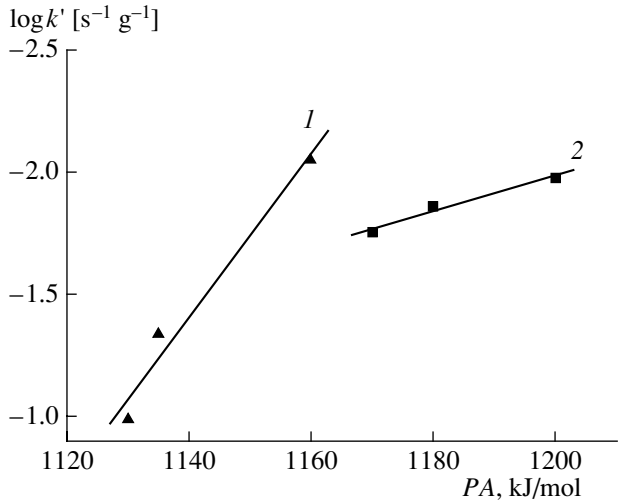

Fig. 7. Rate constant of reaction (I) as a function of the strength of proton sites for (*1*) $Na_xH_{3-x}PW_{12}O_{40}$ (x = 1–3) or (*2*) HZSM-5 zeolites.

bond can be formed because of the π-electron interaction of HPA molecules with surface acidic groups, whereas a strong chemical interaction with basic groups is characteristic of N-CFC(259). In addition, according to electron-microscopic data, the adsorption of $H_3PW_{12}O_{40}$ on N-CFC occurred at the outer surface of a carbon fiber (Fig. 5a). At the same time, the adsorption on CFC-3 can occur either at the outer surface of a fiber (Fig. 5b) or at centers located within the hollow channel of a CFC nanotube. Consequently, the value of a_{ib} for CFC-3 primarily depends on the tubular morphology of fibers (texture characteristics), whereas this value for N-CFC considerably depends on the binding energy of protons of the HPA molecule to basic N-containing groups.

An insignificant difference between the values of $a_{ib}(H_3PW_{12}O_{40})$ and $a_{ib}(Na_3PW_{12}O_{40})$ for N-CFC(259) may be due to the ability of heteropoly anions to form insoluble pyridinium and ammonium salts; this also provides support for the effect of N-containing surface centers on adsorption.

Figure 6 demonstrates the IR spectra of the samples of 8% $H_3PW_{12}O_{40}$/CFC-3 and 10% $H_3PW_{12}O_{40}$/N-CFC(258) supported catalysts prepared by the adsorption method. The IR spectra clearly exhibit absorption bands at 820, 905, 980, and 1075 cm^{-1}. According to published data [7, 40], these bands can be ascribed to the absorption bands of HPAs with the Keggin structure: ν_{as}(W–O_c–W) = 820 cm^{-1}, ν_{as}(W–O_b–W) = 905 cm^{-1}, ν^{as}(W=O_d) = 990 cm^{-1}, and ν_{as}(P–O_a) = 1090 cm^{-1}. Insignificant shifts of bands at 990 and 1090 cm^{-1} could be due to the interaction of the HPA anion with the surface groups of CFC. According to Wu *et al.* [5], additional bands in the regions 1100–1300 and 1400–1600 cm^{-1} can be attributed to C=O vibrations in carbonyl, carboxyl, and lactone groups.

The effect of the pore structure of CFC on adsorption is no less than the effect of the surface chemistry. Thus, a correlation between the values of S_{sp} and a_{max} was observed (Table 1): the values of a_{max} changed symbatically with S_{sp}. These results are consistent with the assumption that multilayer adsorption primarily occurred on the outer surface of the support. It is likely that the adsorption of HPA associates on the outer surface and, probably, in impurity macropores makes a small contribution.

The effect of N-containing surface centers remains unclear. However, experimental data suggest that, in N-CFC samples prepared from reaction mixtures of the same composition (C_5H_5N–H_2) (Table 1) and characterized by approximately equal specific surface areas but different amounts of nitrogen-containing centers, the values of a_{max} referenced to the total nitrogen content of these samples decrease in the following order: N-CFC(301) > N-CFC(259) > N-CFC(258). This order corresponds to the order of increasing concentration of pyridine-like groups. It is likely that this dependence is related to both a decrease in the accessibility of nitrogen-containing centers to HPA molecules and solvation effects, because of which the protonation of pyridine-like groups becomes less favorable than the protonation of amino-like groups [41].

The effect of N-containing surface centers was more pronounced in samples prepared from reaction mixtures of different composition (Table 1). However, the degree of this effect is difficult to evaluate because several parameters undergo simultaneous changes: S_{sp}, D_a, nitrogen content, and the ratio between amino- and pyridine-like groups.

Esterification of n-Butanol with Acetic Acid Catalyzed by $H_3PW_{12}O_{40}$/CFC

The esterification reaction was used [4, 5, 7–9] as a test reaction for comparing the acidities of bulk HPAs and HPAs supported on various carriers. The catalytic activity of bulk HPAs was found to be much higher. Moreover, it was found that the catalytic activity of supported HPAs correlated with the strength of surface acid sites [3].

In this work, we studied the acidic and catalytic properties of the HPA/CFC systems prepared by the adsorption method in reaction (I) of butanol esterification with acetic acid. Reaction (I) was heterogeneous under conditions of our catalytic experiments because (1) the catalyst visually appeared to be an individual solid phase, which could be easily separated from the reaction mass and (2) the reaction did not occur in the reaction mixture filtered from the catalyst. Note that 9–15 wt % HPA supported on CFC was not washed off from the carbon surface into a solution of HOAc even upon boiling for 5 to 6 h.

We found for $H_3PW_{12}O_{40}$/N-CFC(293) that the order of reaction (I) with respect to HPA was close to

Table 3. Esterification of *n*-butanol with acetic acid in the presence of HPA immobilized on various carbon supports

Catalyst	$k \times 10^4$, $s^{-1}\ g^{-1}$	$k' \times 10^4$, $s^{-1}\ g^{-1}$	$k_s \times 10^6$, $s^{-1}\ m^{-2}$	S_{sp}, m^2/g	*PA**, kJ/mol
$H_3PW_{12}O_{40}$**,***	470	470	–	2	1120 ± 20
$NaH_2PW_{12}O_{40}$**	1026	1026	–	3.4	1130
$Na_2HPW_{12}O_{40}$**	462	462	–	3.7	1135
$Na_3PW_{12}O_{40}$**	88	88	–	3.8	1160
HZSM-5 (Al)**	106	126	44.3	402	1170
HZSM-5 (Ga)**	137	137	29.7	461	1180
HZSM-5 (Fe)**	106	126	28.3	375	1200
10% $H_3PW_{12}O_{40}$/N-CFC(301)	15	150	5.3	282	(1175 ± 10)
15% $H_3PW_{12}O_{40}$/N-CFC(259)	45	300	16	283	(1150 ± 10)
10% $H_3PW_{12}O_{40}$/N-CFC(259)	13	130	4.5	283	(1180 ± 10)
10% $H_3PW_{12}O_{40}$/N-CFC(293)	15	150	4.8	309	(1175 ± 10)
10% $H_3PW_{12}O_{40}$/N-CFC(295)	15	150	4.5	324	(1175 ± 10)
10% $H_3PW_{12}O_{40}$/N-CFC(258)	12	120	4.1	290	(1185 ± 10)
10% $H_3PW_{12}O_{40}$/N-CFC(286)	12	120	6.0	201	(1185 ± 10)
10% $NaH_2PW_{12}O_{40}$/N-CFC(286)	7	70	3.5	201	(1205 ± 10)
10% $Na_2HPW_{12}O_{40}$/N-CFC(286)	7	70	3.5	201	(1205 ± 10)
10% $Na_3PW_{12}O_{40}$/N-CFC(286)	3	30	1.5	201	(1245 ± 10)
10% $H_3PW_{12}O_{40}$/N-CFC(122)	15	150	6.3	239	(1175 ± 10)
10% $H_3PW_{12}O_{40}$/N-CFC(141)	16	160	14	110	(1170 ± 10)
9% $H_3PW_{12}O_{40}$/CFC-3	40	444	32	125	(1130 ± 10)
N-CFC(259)	5.9	–	2.1	283	
N-CFC(293)	2.1	–	0.6	309	
CFC-3	0.2	–	0.1	125	

Notes: [BuOH]/[HOAc] = 1 : 15 mol/mol; 80°C; [HPA/C] = 3 wt %.
k' is the reaction rate constant per gram of active component; $k_s = k/S_{sp}$.

* PA values were determined spectroscopically in accordance with the published procedure [42] using pyridine as a probe. The values of PA obtained from the data of catalytic experiments are given in parentheses.

** The catalyst concentration was 0.3 wt %.

*** The reaction temperature was 60°C.

unity, as in the case of bulk HPA, and the activation energies were equal to 22 ± 2 and 30 ± 3 kcal/mol, respectively. Because in the presence of supported HPA, as distinct from bulk HPA, reaction (I) was heterogeneous, it is most likely that the initial step of the reaction is the rapid reversible adsorption of butanol and HOAc followed by reactions at the catalyst surface. This fact may be responsible for the difference in activation energies for $H_3PW_{12}O_{40}$ and $H_3PW_{12}O_{40}$/N-CFC(293).

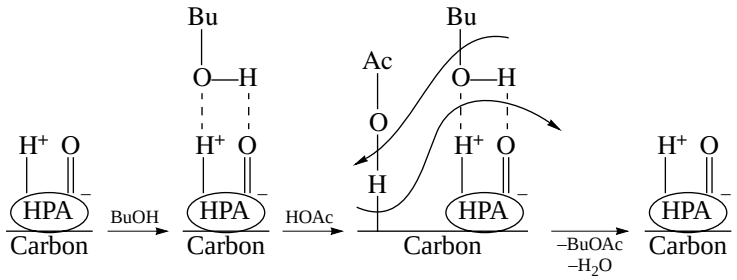

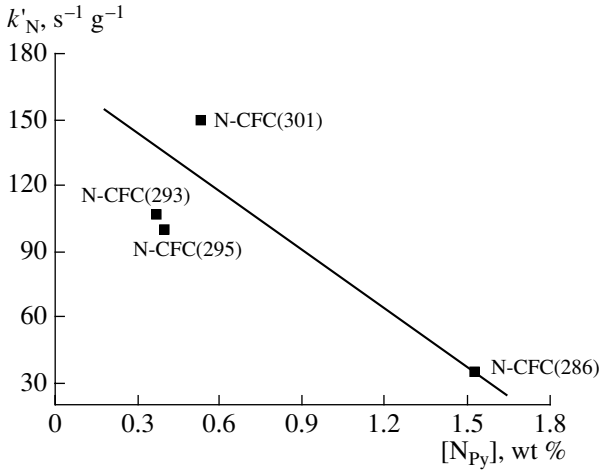

Fig. 8. Effect of the concentration of pyridine-like groups, which are the constituents of filamentous carbon, on the catalytic activity of 10% $H_3PW_{12}O_{40}$/N-CFC in reaction (I) ($k'_N = k'/N$, where N is the total nitrogen amount in grams).

Such behavior was also observed in the dealkylation reaction of 2,6-di-*tert*-butylphenol in the presence of $H_3PW_{12}O_{40}$ and $H_3PW_{12}O_{40}/SiO_2$ [3].

Bulk $H_3PW_{12}O_{40}$ is a strong Brønsted acid, whose strength is greater than that of proton sites in HZSM-5 zeolite [1, 2]. Table 3 summarizes the rate constants k' and k_s of reaction (I), specific surface areas, and strength of acid sites determined as proton affinity (PA) for HZSM-5 zeolites and HPA (bulk and supported on CFC). Figure 7 demonstrates the dependence of the rate of reaction (I) on the strength of the acid sites. Although the reaction was homogeneous in the presence of $Na_xH_{3-x}PW_{12}O_{40}$ (x = 1–3) or heterogeneous in the presence of zeolites, a Brønsted-type correlation was observed in both cases. The strength of acid sites in the HPA/CFC samples was evaluated from kinetic data (with the use of curve *2* in Fig. 7). It was found that the acidity of proton sites decreased upon supporting HPA onto CFC. The strongest sites were detected in the sample of 9% $H_3PW_{12}O_{40}$/CFC-3, whereas the strength of proton sites significantly decreased upon supporting HPA onto N-CFC and became close to the strength of proton sites in HZSM-5 (Al) zeolites (PA = 1170 kJ/mol). It is most likely that the difference in the strength of the acid sites of HPA/CFC-3 and HPA/N-CFC is related to the character and strength of the interaction of HPA proton sites with the surface groups of carbon. The fact that the replacement of $H^+$with Na^+ in the case of $Na_xH_{3-x}PW_{12}O_{40}$/N-CFC resulted in a greater change in the strength of proton sites than in bulk salts (Table 3) is indicative of the strong interaction of HPA with the surface N-groups of the support.

It is well known that catalytic activity increases with increasing HPA concentration on the support surface as a consequence of competition between increasing strength of acid sites and decreasing number of these sites [3]. This is consistent with data obtained in the catalytic tests of 15% $H_3PW_{12}O_{40}$/N-CFC(259) and 10% $H_3PW_{12}O_{40}$/N-CFC(259) samples. An increase in the HPA content from 10 to 15 wt % resulted in an increase in activity by a factor of ~2 and in an increase in the strength of acid sites: PA changed from 1180 ± 10 to 1150 ± 10 kJ/mol (Table 3).

The relationship between the amount of nitrogen-containing centers in a carbon support and the catalytic activity of HPA remains unclear. The nature of nitrogen-containing centers has the greatest effect on the catalytic activity of HPA (Tables 1, 3). Thus, samples with approximately equal specific surface areas and different nitrogen contents exhibited the same activity (10% $H_3PW_{12}O_{40}$/N-CFC(301) and 10% $H_3PW_{12}O_{40}$/N-CFC(295)). However, in the 10% $H_3PW_{12}O_{40}$/N-CFC(141) sample with a high nitrogen content, HPA exhibited greater activity than in the case of other N-CFC supports.

We failed to determine the effect of the nature of N-containing surface centers on the acidic and catalytic properties of HPA because quantitative data on the true chemical composition of the surface of N-CFC are currently unavailable. However, some regularity can be followed. Figure 8 illustrates the effect of the concentration of pyridine-type nitrogen atoms (calculated from XPS data using a peak with E_b = 398.6 ± 0.2 eV) on the catalytic activity of $H_3PW_{12}O_{40}$. It can be seen that the higher the concentration of pyridine-like groups, the lower the catalytic activity of HPA. The strength of the proton sites of the acid decreased in the same order. However, this correlation does not just result from changes in the number of pyridine-like groups because the concentration of amine, aniline, and other nitrogen-containing groups and the ratio between them can change simultaneously.

REFERENCES

1. Misono, M., Mizuno, N., Katamura, K., Kasai, A., Konishi, Y., Sakata, T., Okuhara, T., and Yoneda, Y., *Bull. Chem. Soc. Jpn.*, 1982, vol. 55, p. 400.
2. Kozhevnikov, I.V., *Usp. Khim.*, 1993, vol. 62, no. 5, p. 510.
3. Kozhevnikov, I.V. and Timofeeva, M.N., *J. Mol. Catal.*, 1992, vol. 75, p. 179.
4. Shikata, S., Nakata, S., Okuhara, T., and Misono, M., *J. Catal.*, 1997, vol. 166, p. 263.
5. Wu Yue, Ye Xingkai, Yang Xiangguang, Wang Xinping, Chu Wenling, and Hu Yucai, *Ind. Eng. Chem. Res.*, 1996, vol. 35, p. 2546.
6. Kulikov, S.M., Timofeeva, M.N., Kozhevnikov, I.V., Zaikovskii, V.I., Plyasova, L.M., and Ovsyannikova, I.A., *Izv. Akad. Nauk SSSR, Ser. Khim*, 1989, no. 4, p. 763.
7. Pizzio, L.R., Caceres, C.V., and Blanko, M.N., *Appl. Catal. A*, 1998, vol. 167, p. 283.
8. Chimienti, M.E., Pizzio, L.R., Blanko, M.N., and Caceres, C.V., *Appl. Catal. A*, 2001, vol. 208, p. 7.

9. Levebvre, F., Dupont, P., and Auroux, A., *React. Kinet. Catal. Lett.*, 1995, vol. 55, p. 3.
10. Fenelonov, V.B., *Poristyi uglerod* (Porous Carbon), Novosibirsk: Inst. of Catalysis, 1995, p. 360.
11. Timofeeva, M.N., Matrosova, M.M., Reshetenko, T.V., Avdeeva, L.B., Budneva, A.A., Chuvilinm, A.L., and Likholobov, V.A. *Izv. Akad. Nauk, Ser. Khim.*, 2002, no. 2, p. 232.
12. Stohr, B., Boehm, H.-P., and Schlogl, R., *Carbon*, 1991, vol. 29, no. 6, p. 707.
13. Jansen, R.J.J. and Van Bekkum, H., *Carbon*, 1995, vol. 33, no. 8, p. 1121.
14. Mangun, Ch.L., Benak, K.R., Economy, J., and Foster, K.L., *Carbon*, 2001, vol. 39, no. 12, p. 1809.
15. Vinke, P., van der Eijk, M., Verbree, M., Voskamp, A.F., and van Beccum, H., *Carbon*, 1994, vol. 32, no. 4, p. 675.
16. Li, K., Ling, L., Lu, Ch., Qiao, W., Liu, Zh., Liu, L., and Mochida, I., *Carbon*, 2001, vol. 39, no. 12, p. 1803.
17. Mang, G., Boehm, H.P., Stanczyk, K., and Marsh, H., *Carbon*, 1992, vol. 30, no. 3, p. 391.
18. Terrones, M., Redlich, Ph., Grobert, N., Trasobares, S., Hsu, W.K., Terrones, H., Zhu, Y.Q., Hare, J.P., Cheetham, A.K., Ruhle, M., Kroto, H.W., and Walton, D.R.M., *Adv. Mater.*, 1999, vol. 11, p. 655.
19. Terrones, M., Terrones, H., Grobert, N., Hsu, W.K., Zhu, Y.Q., Hare, J.P., Kroto, H.W., Walton, D.R.M., Kohler-Redlich, Ph., Ruhle, M., Zhang, J.P., and Cheetham, A.K., *Appl. Phys. Lett.*, 1999, vol. 75, no. 25, p. 3932.
20. Nakajima, T. and Koh, M., *Carbon*, 1997, vol. 35, no. 2, p. 203.
21. RF Patent 2147925, 2000.
22. Kvon, R.I., Il'inich, G.N., Chuvilin, A.L., and Likholobov, V.A., *J. Mol. Catal., A: Chem.*, 2000, vol. 158, p. 413.
23. Pels, J R., Kapteijn, F., Moulijn, J.A., Zhu, Q., Thomas, K.M., *Carbon*, 1995, vol. 33, no. 11, p. 1641.
24. Stanczyk, K., Dziembaj, R., Pivovarska, Z., and Witkowski, St., *Carbon*, 1995, vol. 33, no. 10, p. 1383.
25. Schmiers, H., Friebel, J., Streubel, P., Hesse, R., and Kopsel, R., *Carbon*, 1999, vol. 37, p. 1965.
26. Strelko, V.V., Kuts, V.S., and Throver, P.A., *Carbon*, 2000, vol. 38, no. 10, p. 1499.
27. Singoredjo, L., Kapteijn, F., Moulijn, J.A., Martin-Martinez, J.-M., and Boehm, H.-P., *Carbon*, 1993, vol. 31, no. 1, p. 213.
28. Rivera-Utrilla, J. and Ferro-Garcia, M.A., *Adsorpt. Sci. Technol.*, 1986, vol. 3, p. 293.
29. Drozdetskii, A.G., Radushev, A.V., Grishin, V.M., and Turbin, A.S., *Zh. Prikl. Khim.*, 1997, vol. 70, no. 9, p. 1529.
30. Avdeeva, L.B., Reshetenko, T.V., Ismagilov, Z.R., and Likholobov, V.A., *Appl. Catal., A*, 2002, vol. 228, p. 53.
31. Downs, W.B. and Baker, R.T.K., *Carbon*, 1991, vol. 29, no. 8, p. 1173.
32. Moulder, J.F., Stickle, W.F., Sobol, P.E., and Bomben, K.D., *Handbook of X-Ray Spectroscopy*, Chastain, Y., and den Prairie, E., Eds., Eden Prairie: Perkin–Elmer, 1979.
33. Song, W., Venimadhavan, G., Manning, J.M., and Malone, M.F., *Ind. Eng. Chem. Res.*, 1998, vol. 37, no. 5, p. 1917.
34. Nagaraju, N., Peeran, M., and Prasad, D., *React. Kinet. Catal. Lett.*, 1997, vol. 61, no. 1, p. 155.
35. Chu, W., Yang, X., Ye, X., and Wu, Y., *Chin. J. Catal.*, 1997, vol. 88, no. 3, p. 225.
36. Xiong, Z., Song, D., and Feng, R., *Huaxue Shije*, 1992, vol. 33, no. 7, p. 303.
37. Zhao, N., Gong, L., and Li, J., *Gaodeng Xuexiao Huaxue Xuebao*, 1992, vol. 13, no. 9, p. 1263.
38. Fomkin, A.A., Regent, N.I., and Sinitsyn, V.I., *Izv. Akad. Nauk, Ser. Khim.*, 2000, no. 6, p. 1018.
39. Tarkovskaya, I.A., *Okislennyi ugol'* (Oxidized Coal), Kiev: Naukova Dumka, 1981, p. 197.
40. Trolliet, C., Coudurier, G., and Vedrine, J.C., *Top. Catal.*, 2001, no. 15, p. 73.
41. Kabachkin, M.I., *Usp. Khim.*, 1979, no. 9, p. 1524.
42. Paukshtis, E.A., *Infrakrasnaya spektroskopiya v geterogennom kislotno-osnovnom katalize* (Infrared Spectroscopy in Heterogeneous Acid–Base Catalysis), Novosibirsk: Nauka, 1992, p. 125.